Monte Carlo Study of Electron Transport in Strained Silicon Inversion Layers

E. Ungersboeck and H. Kosina

Institute for Microelectronics, TU Vienna, Gußhausstraße 27–29/E360, 1040 Wien, Austria
Phone: +43-1-58801/36022, Fax: +43-1-58801/36099, E-mail: ungersboeck@iue.tuwien.ac.at

During the last years the introduction of strain in the channel of Si MOSFETs has become a widely used technique to improve transistor drive currents. Strain can be induced by epitaxially growing thin Si layers on $Si_{1-y}Ge_y$, or alternatively by processing additional cap layers over the transistors. The latter method is especially interesting for industry because it requires only a slight modification of the process flow.

Surprisingly, from a theoretical viewpoint the mobility enhancement caused by strain is still an issue of discussion. It was claimed that using the well established models for scattering in the 2DEG (two dimensional electron gas) the mobility gain of SSi (strained Si) at low effective fields should be overwhelmed by more pronounced surface roughness scattering at large effective fields [1]. Due to this fact, only with the assumption of much smoother interfaces of SSi one should be able to get qualitative agreement with experimental data. Even though it seemed to be unphysical to change the smoothness of the strained Si-SiO_2 interface the Monte Carlo community has adopted this assumption.

The purpose of this work is twofold: First we investigate how to efficiently implement the Pauli principle in a one-particle Monte Carlo method. Having settled for a correct method the mobility of strained inversion layers is calculated adopting scattering models from [2]. Our simulation results show that the effective mobility of SSi is larger than that of unstrained Si even at high effective fields without having to change the surface roughness parameters. A mobility enhancement up to 50% depending on the level of strain is observed.

A one-dimensional Schrödinger-Poisson solver [3] is used with modifications to account for the energy splitting between the twofold and the fourfold conduction-band minima and for the change of the band-gap. The resulting subband energies for a surface in {001} orientation are plotted in Fig. 1. The matrix elements for phonon and surface-roughness scattering are calculated following [2]. Values for the correlation length $\Lambda = 1.3$ nm and step height $\Delta = 0.4$ nm were adopted from [1]. Coulomb scattering has been ignored as we mainly focus on the high effective field region. The dielectric function was treated as a tensor quantity and not as a scalar function as the latter approximation is only valid for ideal 2D systems where the wave functions have a δ-like shape. Furthermore the plasma dispersion function was not used to calculate the polarization function, as the plasma dispersion function underestimates the polarization function in the degenerate case. A non-parabolic bandstructure ($\alpha = 0.5$ eV^{-1}) was used leading to a 20% reduction of the phonon-limited mobility at 300 K in agreement with [1].

It is well known that in the limit of vanishing driving fields the Kubo-Greenwood formula can be used to calculate the mobility. We tested several Monte Carlo algorithms in the zero-field limit and were thus able to show that a non-selfconsistent implementation of an algorithm proposed by Bosi and Jacoboni [4] and a more recent algorithm proposed by Yamakawa [5] deviate from the Kubo-Greenwood mobility. Thus an efficient zero-field bulk MC algorithm taking into account degeneracy effects [6] was adapted for the subband MC simulator. The resulting mobility curves stemming from the above mentioned algorithms are plotted in Fig. 1. The largest discrepancy is observed in a method (label B in Fig. 1), where the Pauli blocking factor $1 - f(k)$ is approximated using the equilibrium distribution function $f_0(k)$. This implementation can be shown to lead to unphysical subband populations, kinetic energies, and mobilities. The reason being that at high degeneracy the error $\Delta(k) = f(k) - f_0(k)$ becomes dominant rather than negligible.

By means of MC simulations we can deduce the effect of degeneracy both on the phonon-limited mobility and the effective mobility including surface-roughness scattering. Fig. 2 shows that in the unstrained case the inclusion of the Pauli principle has almost no impact on the effective mobility, whereas degeneracy effects increase the effective mobility of strained inversion layers at high inversion layer concentrations. This can be understood from the following: When using non-degenerate statistics electrons reside at lower kinetic energies and hence experience more effective surface-roughness scattering. On the other hand side, having lower kinetic energies, phonon scattering is less pronounced. In unstrained Si these two effects cancel each other, and the difference between a simulation with non-degenerate and degenerate statistics is very small even for high effective fields. In strained Si, where the ratio between phonon- and surface roughness scattering is different – due to suppressed intervalley transitions – simulations with degeneracy effects yield higher mobilities.

Our simulation results in Fig. 3 for biaxially strained Si on $Si_{1-y}Ge_y$ inversion layer mobility for various Ge contents suggest a saturation of the mobility enhancement at $y \approx 25\%$. The anomalous intersection of the strained and unstrained mobility curve from [1] was not observed, however, the predicted mobility for SSi is still underestimated.

This work has been partly supported by the European Commission, project SINANO, IST 506844.

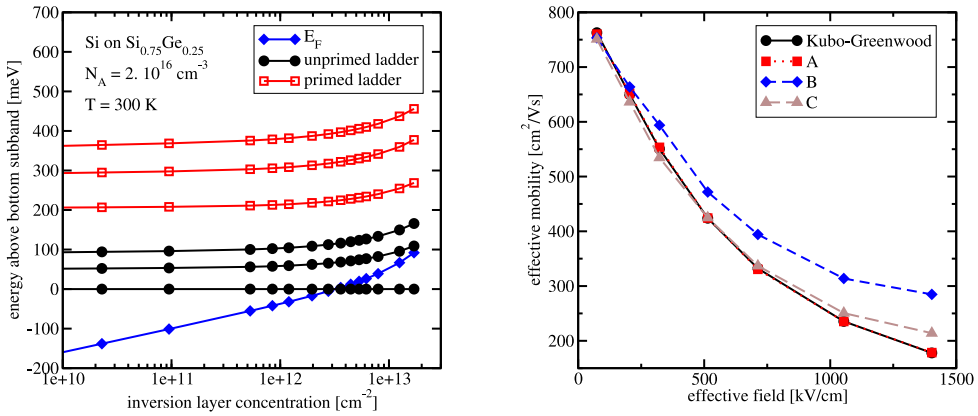

Figure 1: Left graph: Calculated subband energies for a {001} oriented substrate measured from the energy of the lowest unprimed subband. Right graph: Comparison of zero-field mobility calculated using the Kubo-Greenwood formula (black circles), an adapted algorithm from [6] (label A), a non-selfconsistent implementation of a method proposed by [4] (label B), and the method proposed by [5] (label C).

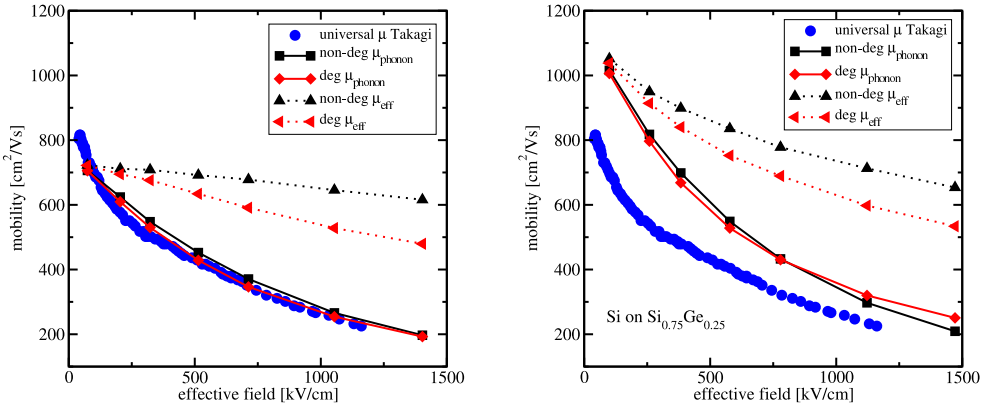

Figure 2: Calculated phonon-limited and effective mobility compared to the universal mobility curve with and without degeneracy effects for unstrained Si (left graph) and biaxially strained Si (right graph).

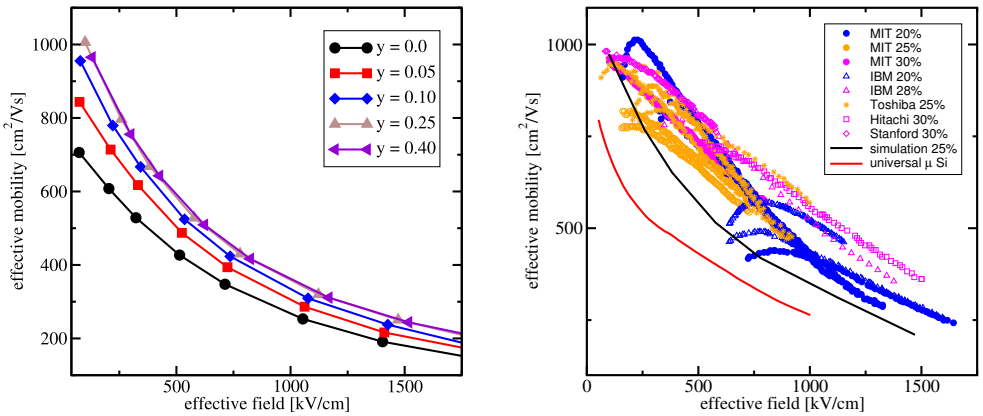

Figure 3: Left graph: Simulation results for the mobility of biaxially strained Si on $Si_{1-y}Ge_y$ for various Ge contents. Right graph: Comparison with experimental data.

REFERENCES

[1] M. V. Fischetti, F. Gamiz, and W. Hänsch, J.Appl.Phys. **92**, 7320 (2002).
[2] C. Jungemann, A. Edmunds, and W. L. Engl, Solid-State Electron. **36**, 1529 (1993).
[3] D. Vasileska and Z. Ren, *SCHRED 2.0 User's Manual*, http://www.nanohub.org, 2000.
[4] S. Bosi and C. Jacoboni, J. Phys. C: Solid State Phys. **9**, 315 (1976).
[5] S. Yamakawa *et al.*, J.Appl.Phys. **79**, 911 (1996).
[6] S. Smirnov, H. Kosina, M. Nedjalkov, and S. Selberherr, J.Appl.Phys. **94**, 5791 (2003).